

Experiments and modelling of high power impulse magnetron sputtering discharges with metallic target

J. T. Guðmundsson^{1,2}, K. Barynova¹, S. Suresh Babu¹, M. Rudolph³, J. Fischer⁴, Tetsuhide Shimizu⁴, and D. Lundin⁴

¹ Science Institute, University of Iceland, Reykjavik, Iceland

² KTH Royal Institute of Technology, Stockholm, Sweden

³ Leibniz Institute of Surface Engineering (IOM), Leipzig, Germany

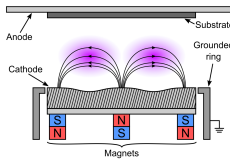
⁴ Plasma and Coatings Physics, Linköping University, Sweden

⁵ Tokyo Metropolitan University, Tokyo, Japan

68th Annual SVC Technical Conference
Nashville, Tennessee

May 22, 2025

Introduction – Magnetron sputtering



Gudmundsson and Lundin (2020) in High Power Impulse Magnetron Sputtering Discharge, Elsevier, 2020

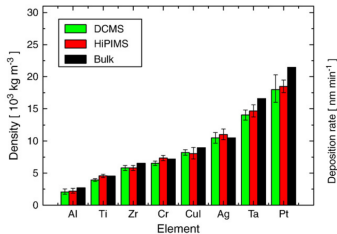
- Magnetron sputtering has been a highly successful technique that is essential in a number of industrial applications
- In a high power impulse magnetron sputtering (HiPIMS) the discharge is driven by high power pulses of low repetition frequency, and with low duty cycle
- This results in high discharge current density, increased electron density, and increased ionization of the sputtered species

Gudmundsson (2020) PSST 29 113001

Gudmundsson et al. (2012) JVSTA 30 030801

Introduction – Magnetron sputtering

- The film mass density is always higher when deposited with HiPIMS
- The films typically exhibit better crystallinity, and overall improved film properties
- There is a drawback: The deposition rate is lower for HiPIMS when compared to dcMS operated at the same average power
- Many of the ions of the target material are attracted back to the target surface by the cathode potential



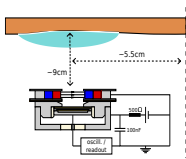
From Samuelsson et al. (2010) SCT 202 591

Overview

- Ionized flux fraction – measurements
- The ionization region model (IRM)
- Deposition rate vs ionized flux fraction
- Working gas rarefaction
- Summary

Ionized flux fraction – measurements

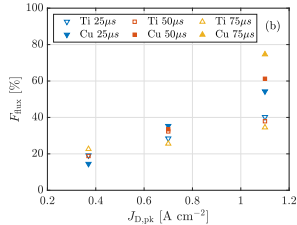
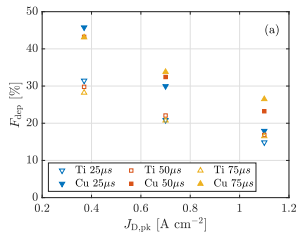
Ionized flux fraction – measurements



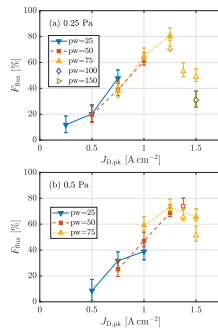
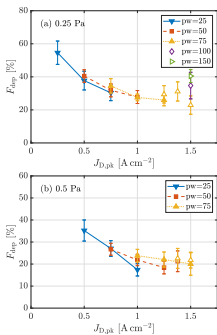
- The ionized flux fraction and the deposition rate fraction – measured by an ion meter in HiPIMS discharges with Cu and Ti targets and working gas pressure of 0.3 Pa

Cu: Fischer et al. (2023) PSST **32** 125006

Ti: Shimizu et al. (2021) PSST **30** 045006



Ionized flux fraction – measurements



From Fischer et al. (2023) PSST 32 125006

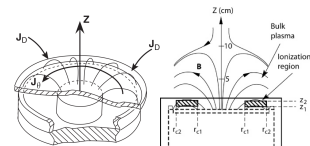
- The measured normalized deposition rate (left) and ionized flux fraction (right) as a function of the peak discharge current density $J_{D,\text{peak}}$ for working gas pressure of (a) 0.25 Pa and (b) 0.5 Pa

The ionization region model (IRM)

Ionization region model

- The ionization region model (IRM) is a time-dependent volume averaged plasma chemical model of the ionization region (IR) of the HiPIMS discharge
- The IRM gives the temporal evolution of the densities of ions, neutrals and electrons
- The IRM gives also two internal parameters that are of importance
 - α_t – ionization probability
 - β_t – back-attraction probability

Detailed model description is given in Huo et al. (2017) JPD **50** 354003



The definition of the volume covered by the IRM

- The IR is defined as an annular cylinder of width $w_{rt} = r_{c2} - r_{c1}$ and thickness $L = z_2 - z_1$, extends from z_1 to z_2 axially away from the target



Ionization region model

- The temporal development is defined by a set of ordinary differential equations giving the first time derivatives of
 - the electron energy
 - the particle densities for all the particles (except electrons)
- The species assumed in the non-reactive-IRM are
 - cold electrons e^C , hot electrons e^H
 - argon atoms $Ar(3s^23p^6)$, warm argon atoms in the ground state Ar^W , hot argon atoms in the ground state Ar^H , Ar^m ($1s_5$ and $1s_3$) (11.6 eV), argon ions Ar^+ (15.76 eV), doubly ionized argon ions Ar^{2+} (27.63 eV)
 - Metal atoms, sometimes metastable states, metal ion M^+ , and doubly ionized metal ions M^{2+}

Detailed model description is given in Huo et al. (2017) JPD 50 354003

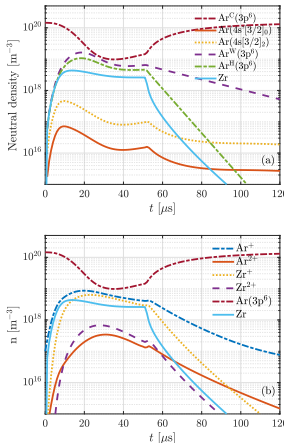
Ionization region model

- As an example the particle balance equation for the metal ion M^+ is

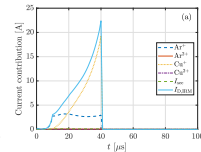
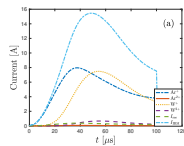
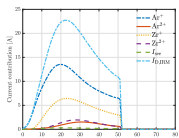
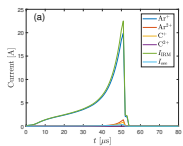
$$\frac{dn_{M^+}}{dt} = \underbrace{k_{iz,M}^c n_{e,c} n_M + k_{iz,M}^h n_{e,h} n_M}_{\text{electron impact ionization}} + \underbrace{k_{P,iz} n_{Ar^m} n_M}_{\text{Penning ionization}} \\ + \underbrace{k_{chexc,1} n_M n_{Ar^+} + k_{chexc,2} n_{M^{2+}} n_{Ar}}_{\text{charge exchange}} - \underbrace{k_{iz,M^+}^c n_{e,c} n_{M^+} - k_{iz,M^+}^h n_{e,h} n_{M^+}}_{\text{electron impact ionization to create } M^{2+}} \\ - \underbrace{\frac{\Gamma_{M^+}^{RT} + \Gamma_{M^+}^{BP} (S_{IR} - S_{RT})}{\mathcal{V}_{IR}}}_{\text{ion flux out of the ionization region}}$$

Ionization region model studies of HiPIMS

- The temporal evolution of the neutral and ion densities in a discharge with zirconium target
- Ar^+ ions dominate the discharge – but Zr^+ ions are not far off
- Ar^{2+} and Zr^{2+} ions have much lower densities
- Working gas rarefaction is very apparent



Ionization region model



C: PSST (2021) **30** 115017 Zr: JVSTA (2024) **42** 043007 W: PSST (2022) **31** 065009 Cu: SCT (2022) **442** 128189

- The temporal evolution of the discharge current composition at the target surface for four different targets
- With Cu target Cu^+ ions dominate, with graphite target Ar^+ ions dominate
- For Zr and W targets there is a mix of Ar^+ and metal ions

Deposition rate vs ionized flux fraction

Deposition rate – α_t and β_t

- We can relate the measured quantities normalized deposition rate $F_{\text{DR,sput}}$ and the ionized flux fraction $F_{\text{ti,flux}}$

$$F_{\text{DR,sput}} = \frac{\Gamma_{\text{DR}}}{\Gamma_0} = (1 - \alpha_t \beta_t)$$

$$F_{\text{ti,flux}} = \frac{\Gamma_{\text{DR,ions}}}{\Gamma_{\text{DR,sput}}} = \frac{\Gamma_0 \alpha_t (1 - \beta_t)}{\Gamma_0 (1 - \alpha_t \beta_t)} = \frac{\alpha_t (1 - \beta_t)}{(1 - \alpha_t \beta_t)}$$

to the internal parameters back attraction probability β_t

$$\beta_t = \frac{1 - F_{\text{DR,sput}}}{1 - F_{\text{DR,sput}}(1 - F_{\text{ti,flux}})}$$

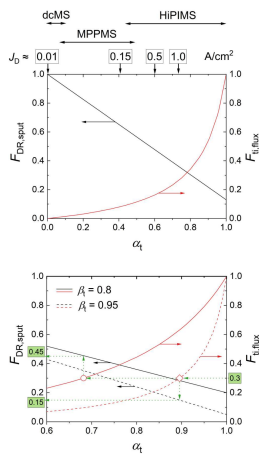
and ionization probability α_t

$$\alpha_t = 1 - F_{\text{DR,sput}}(1 - F_{\text{ti,flux}})$$



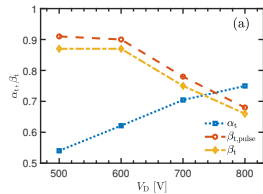
Deposition rate – Optimization

- There are two measures of how good a HiPIMS discharge is:
 - the fraction $F_{\text{DR,sput}}$ of all the sputtered material that reaches the diffusion region (DR)
 - the fraction $F_{\text{ti,flux}}$ of ionized species in that flux
- There is a trade off between the goals of higher $F_{\text{DR,sput}}$ and higher $F_{\text{ti,flux}}$
- The question that remains:
 - How can we vary the ionization probability α_t and maybe more importantly the back-attraction probability β_t ?



Deposition rate vs ionized flux fraction – α_t and β_t

- The internal discharge parameters α_t and β_t from the ionization region model (IRM)
- For tungsten target the ionization probability α_t increases with increased discharge voltage or increased discharge current density
- The peak discharge current increases with increased discharge voltage
- The back-attraction probability $\beta_{t,pulse}$ decreases with increased discharge voltage

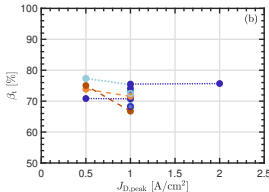
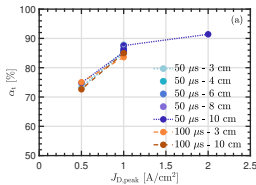
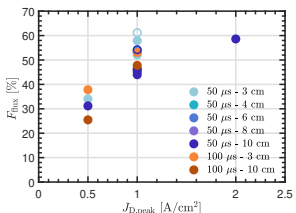


A discharge with a tungsten target

From Suresh Babu et al. (2022) PSST 31 065009

Deposition rate vs ionized flux fraction – α_t and β_t

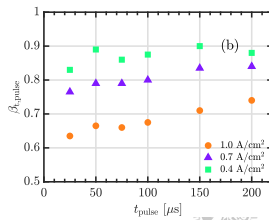
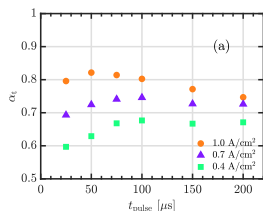
- For zirconium target the ionization probability α_t increases with increased current density
- The back-attraction probability $\beta_{t,pulse}$ does not show any trend



- The measured ionized flux fraction is used to lock the model

Deposition rate vs ionized flux fraction – α_t and β_t

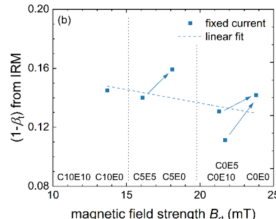
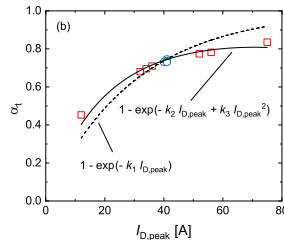
- For chromium target the ionization probability α_t increases with increased current density and
- The back-attraction probability $\beta_{t,pulse}$ decreases with increased peak discharge current density and with decreasing pulse length



Deposition rate vs ionized flux fraction – α_t and β_t

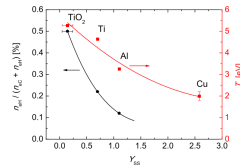
- The ionization probability α_t increases with increased discharge current
- The ion escape fraction $(1 - \beta_t)$ versus the magnetic field strength

From Rudolph et al. (2022) JPD **55** 015202

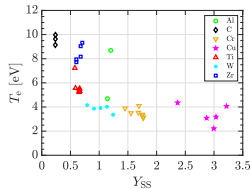


Deposition rate vs ionized flux fraction – α_t and β_t

- We know that the electron temperature and the hot electron density fall with increased sputter yield
- Held *et al.* observed that titanium atoms are ionized within 0.5 mm from the target surface (high $\beta_{t,pulse}$), while aluminum and chromium atoms can travel further before being ionized (lower $\beta_{t,pulse}$)
- The measured electron temperature is 4.5 eV for titanium target compared to 2.6 eV (aluminum) and 1.5 eV (chromium)

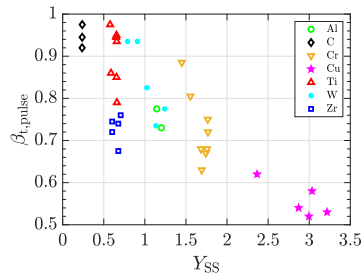


From Brenning et al. (2017) PSST **26** 125003



Deposition rate vs ionized flux fraction – α_t and β_t

- What determines the back-attraction probability ?
- How can one influence the back-attraction probability ?
- The back-attraction probability $\beta_{t,pulse}$, determined by IRM, versus the self-sputter yield for various target materials
- The data indicate that the back-attraction probability decreases roughly linearly with increased self-sputter yield

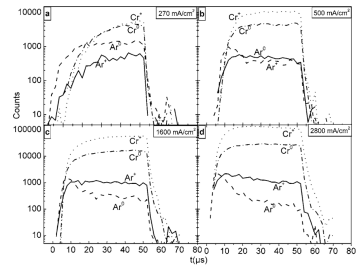


From Barynova et al. (2025) PSST submitted

Working gas rarefaction

Working gas rarefaction

- The sputtered species enter the discharge at considerable energy, which is determined by the cohesive energy of the solid target
- The interaction between the energetic sputtered particles and the working gas atoms can lead to a reduction in the working gas density – as has been observed experimentally in the HiPIMS discharge
- Working gas rarefaction has been observed in the HiPIMS discharge



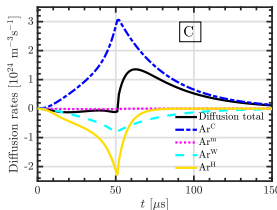
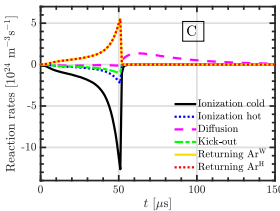
From Alami et al. (2006) APL **89**(15) 154104

Working gas rarefaction

- HiPIMS discharge with graphite target and $J_{D,\text{peak}} = 1 \text{ A cm}^{-2}$

Eliasson et al. (2021) PSST **30** 115017

- Argon atoms are lost mainly through electron impact ionization by primary and secondary electrons
- Contributions of kick-out and charge-exchange are negligible
- Diffusion contributes to a net loss of argon atoms during the pulse, but to a flow into the ionization region after the pulse is off

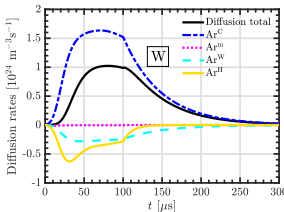
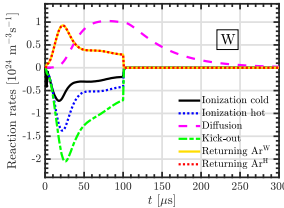


Working gas rarefaction

- HiPIMS discharge with tungsten target and $J_{D,\text{peak}} = 0.54 \text{ A cm}^{-3}$

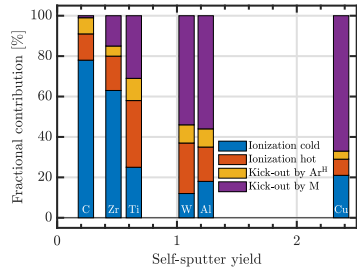
Suresh Babu et al. (2022) PSST 31 065009

- The main contributor to the loss of argon atoms from the IR is kick-out by tungsten atoms sputtered from the target (39 – 48 % contribution)
- The second most important loss process is electron impact ionization by secondary electrons followed by electron impact ionization by the primary electrons



Working gas rarefaction

- The relative contributions of the various processes to working gas rarefaction varies greatly depending on the target material
- The various contributions versus the atomic mass of the target material for $J_{D,\text{peak}} \sim 1 \text{ A/cm}^2$ and $p_g \sim 1 \text{ Pa}$



From Barynova et al. PSST 33(6) 065010

Summary

Summary

- The discharge current composition at the target surface depends on the target material
- There is an inescapable conflict between the goals of higher deposition rate and higher fraction of ionized species in the sputtered material flux
- The back-attraction probability appears to depend on the self-sputter yield – it is lower for higher self-sputter yield
- The main contributor to working gas rarefaction for low sputter yield target is electron impact ionization, while for targets with high sputter yield kick-out by the sputtered species is the main contributor

Thank you for your attention

tumi@hi.is

The slides can be downloaded at

<http://langmuir.raunvis.hi.is/~tumi/ranns.html>

Further reading

- J. T. Gudmundsson, Physics and technology of magnetron sputtering discharges, *Plasma Sources Science and Technology*, **29**(11) (2020) 113001
- J. T. Gudmundsson, André Anders, and Achim von Keudell, Foundations of physical vapor deposition with plasma assistance, *Plasma Sources Science and Technology*, **31**(8) (2022) 083001
- Daniel Lundin, Tiberiu Minea and Jon Tomas Gudmundsson (eds.), *High Power Impulse Magnetron Sputtering: Fundamentals, Technologies, Challenges and Applications*, Elsevier, 2020



References

- Alami, J., K. Sarakinos, G. Mark, and M. Wuttig (2006). On the deposition rate in a high power pulsed magnetron sputtering discharge. *Applied Physics Letters* 89(15), 154104.
- Barynova, K., N. Brenning, S. Suresh Babu, J. Fischer, D. Lundin, M. A. Raadu, J. T. Gudmundsson, and M. Rudolph (2025). Self-regulating electron temperature in high-power impulse magnetron sputtering discharges and its effect on the metal ion escape. *Plasma Sources Science and Technology*, submitted for publication.
- Barynova, K., S. Suresh Babu, M. Rudolph, J. Fischer, D. Lundin, M. A. Raadu, N. Brenning, and J. T. Gudmundsson (2024). On working gas rarefaction in high power impulse magnetron sputtering. *Plasma Sources Science and Technology* 33(6), 065010.
- Brenning, N., A. Butler, H. Hajihoseini, M. Rudolph, M. A. Raadu, J. T. Gudmundsson, T. Minea, and D. Lundin (2020). Optimization of HiPIMS discharges: The selection of pulse power, pulse length, gas pressure, and magnetic field strength. *Journal of Vacuum Science and Technology A* 38(3), 033008.
- Brenning, N., J. T. Gudmundsson, M. A. Raadu, T. J. Petty, T. Minea, and D. Lundin (2017). A unified treatment of self-sputtering, process gas recycling, and runaway for high power impulse sputtering magnetrons. *Plasma Sources Science and Technology* 26(12), 125003.
- Eliasson, H., M. Rudolph, N. Brenning, H. Hajihoseini, M. Zanáška, M. J. Adriaans, M. A. Raadu, T. M. Minea, J. T. Gudmundsson, and D. Lundin (2021). Modeling of high power impulse magnetron sputtering discharges with graphite target. *Plasma Sources Science and Technology* 30(11), 115017.
- Fischer, J., M. Renner, J. T. Gudmundsson, M. Rudolph, H. Hajihoseini, N. Brenning, and D. Lundin (2023). Insights into the copper HiPIMS discharge: Deposition rate and ionised flux fraction. *Plasma Sources Science and Technology* 32(12), 125006.
- Gudmundsson, J. T. (2020). Physics and technology of magnetron sputtering discharges. *Plasma Sources Science and Technology* 29(11), 113001.
- Gudmundsson, J. T., N. Brenning, D. Lundin, and U. Helmersson (2012). The high power impulse magnetron sputtering discharge. *Journal of Vacuum Science and Technology A* 30(3), 030801.
- Gudmundsson, J. T. and D. Lundin (2020). Introduction to magnetron sputtering. In D. Lundin, T. Minea, and J. T. Gudmundsson (Eds.), *High Power Impulse Magnetron Sputtering: Fundamentals, Technologies, Challenges and Applications*, pp. 1–48. Amsterdam, The Netherlands: Elsevier.

References

- Hajihoseini, H., M. Čada, Z. Hubička, S. Ünalıdi, M. A. Raadu, N. Brenning, J. T. Gudmundsson, and D. Lundin (2019). The effect of magnetic field strength and geometry on the deposition rate and ionized flux fraction in the HiPIMS discharge. *Plasma* 2(2), 201–221.
- Held, J., V. Schulz-von der Gathen, and A. von Keudell (2023). Ionization of sputtered material in high power impulse magnetron sputtering plasmas – comparison of titanium, chromium and aluminum. *Plasma Sources Science and Technology* 32(6), 065006.
- Helmersson, U., M. Lattemann, J. Alami, J. Bohlmark, A. P. Ehiasarian, and J. T. Gudmundsson (2005). High power impulse magnetron sputtering discharges and thin film growth: A brief review. In *Proceedings of the 48th Society of Vacuum Coaters Annual Technical Conference*, pp. 458 – 464.
- Huo, C., D. Lundin, J. T. Gudmundsson, M. A. Raadu, J. W. Bradley, and N. Brenning (2017). Particle-balance models for pulsed sputtering magnetrons. *Journal of Physics D: Applied Physics* 50(35), 354003.
- Magnus, F., A. S. Ingason, S. Olafsson, and J. T. Gudmundsson (2012). Nucleation and resistivity of ultrathin TiN films grown by high power impulse magnetron sputtering. *IEEE Electron Device Letters* 33(7), 1045 – 1047.
- Raadu, M. A., I. Axnäs, J. T. Gudmundsson, C. Huo, and N. Brenning (2011). An ionization region model for high power impulse magnetron sputtering discharges. *Plasma Sources Science and Technology* 20(6), 065007.
- Rudolph, M., N. Brenning, H. Hajihoseini, M. A. Raadu, T. M. Minea, A. Anders, D. Lundin, and J. T. Gudmundsson (2022). Influence of the magnetic field on the discharge physics of a high power impulse magnetron sputtering discharge. *Journal of Physics D: Applied Physics* 55(1), 015202.
- Rudolph, M., H. Hajihoseini, M. A. Raadu, J. T. Gudmundsson, N. Brenning, T. M. Minea, A. Anders, and D. Lundin (2021). On how to measure the probabilities of target atom ionization and target ion back-attraction in high-power impulse magnetron sputtering. *Journal of Applied Physics* 129(3), 033303.
- Samuelsson, M., D. Lundin, J. Jensen, M. A. Raadu, J. T. Gudmundsson, and U. Helmersson (2010). On the film density using high power impulse magnetron sputtering. *Surface and Coatings Technology* 202(2), 591–596.

References

- Shimizu, T., M. Zanáška, R. P. Viljoan, N. Brenning, U. Helmersson, and D. Lundin (2021). Experimental verification of deposition rate increase, with maintained high ionized flux fraction, by shortening the HiPIMS pulse. *Plasma Sources Science and Technology* 30(4), 045006.
- Suresh Babu, S., M. Rudolph, D. Lundin, T. Shimizu, J. Fischer, M. A. Raadu, N. Brenning, and J. T. Gudmundsson (2022). Ionization region model of a high power impulse magnetron sputtering of tungsten. *Plasma Sources Science and Technology* 31(6), 065009.
- Suresh Babu, S., J. Fischer, M. Rudolph, D. Lundin, and J. T. Gudmundsson (2024). Modeling of high power impulse magnetron sputtering discharges with a zirconium target. *Journal of Vacuum Science and Technology A* 42(4), 043007.